



Published in final edited form as:

Ann Biomed Eng. 2008 May ; 36(5): 821–830.

Radiation-Guided P-Selectin Antibody Targeted to Lung Cancer

G. Hariri¹, Y. Zhang¹, A. Fu¹, Z. Han¹, M. Brechbiel², M. N. Tantawy³, T. E. Peterson³, R. Mernaugh⁴, and D. Hallahan^{1,4}

¹Department of Radiation Oncology, Vanderbilt University Medical Center, Nashville, TN 37232, USA

²National Cancer Institute, Center for Cancer Research, Bethesda, MD 20892, USA

³Department of Radiology and Radiological Sciences, Vanderbilt University Institute of Imaging Science, Vanderbilt University, Nashville, TN 37232, USA

⁴Vanderbilt Ingram Cancer Center, Vanderbilt University, Nashville, TN 37232, USA

Abstract

Purpose—P-selectin expression is significantly increased in tumor microvasculature following exposure to ionizing radiation. The purpose of this study was to image radiation-induced P-selectin expression *in vivo* using optical imaging and gamma camera imaging in a heterotopic lung cancer model by using ScFv antibodies to P-selectin.

Procedures—*In vitro* studies using endothelial cells were done using 3 Gy radiation and selected ScFv antibodies to P-selectin. *In vivo* studies were performed using Lewis lung carcinoma cells subcutaneously injected into the hind limbs of nude mice. Mice were treated with 6 Gy radiation and sham radiation 10 days post-inoculation. P-selectin expression was assessed with near-infrared imaging using Cy7 labeled antibody, and gamma camera imaging using ¹¹¹In-DTPA labeled antibody.

Results—*In vitro* studies showed antibody binding to P-selectin in radiation treated endothelial cells. *In vivo* optical imaging and gamma camera imaging studies showed significant tumor-specific binding to P-selectin in irradiated tumors compared to unirradiated tumors.

Conclusions—Optical imaging and gamma camera imaging are effective methods for visualizing *in vivo* targeting of radiation-induced P-selectin in lung tumors. This study suggests that fluorescent-labeled and radiolabeled ScFv antibodies can be used to target radiation-induced P-selectin for the tumor-specific delivery of therapeutic drugs and radionuclides *in vivo*.

Keywords

P-selectin; Radiation; Lung cancer; Optical imaging; Nuclear imaging

INTRODUCTION

Current treatments for cancer rely on systemic administration of chemotherapeutic drugs with the goal of maximizing damage to tumor cells despite exposure and toxicity to healthy tissues. This approach is beneficial for damaging tumor tissue but due to the many side effects of these cytotoxic drugs, healthy tissues can be damaged and organ function can be compromised. Targeted delivery of drugs to tumors attempts to improve the bioavailability of drugs at the tumor site while reducing systemic toxicity to healthy organs and tissues. The efficacy of traditional cytotoxic cancer therapies comes with the price of significant toxicity to normal

Address correspondence to D. Hallahan, Department of Radiation Oncology, Vanderbilt University Medical Center, Nashville, TN 37232, USA. Electronic mail: dennis.hallahan@vanderbilt.edu.

cells, which can limit the success of therapy. Greater understanding of the molecular differences between cancer cells and normal cells has led to the development of therapies that target cancer cells, including antibodies targeted at tumor associated antigens. The targeted nature of such therapies offers the promise of greater efficacy and less toxicity, and potentially greater treatment success.

Vascular Targeting

Tumor angiogenesis is recognized as essential for the growth and progression of all tumor types, therefore, targeting the delivery of cytotoxic and radiosensitizing drugs to tumor blood vessels is an important approach in the treatment of cancer. The lumen of tumor microvasculature is composed of a monolayer of endothelial cells that controls vascular tone, blood flow and extravasation of components from the bloodstream.²¹ This microvascular tissue plays an essential role in the process of inflammation and is affected by radiation therapy used in many cancer treatments. Radiation therapy is typically used to treat tumors locally, but it can also be used to “guide” drugs to specific sites by creating localized areas of inflammation and inducing the expression of radiation-specific receptors in tumors, including P-selectin.^{11,13} Studies have shown that ionizing radiation causes oxidative injury in endothelial cells, which in turn respond by activating the process of inflammation and platelet aggregation through cell adhesion molecules (CAMs).^{1,9,12,33} These molecules include ICAM-1, VCAM, integrins, and selectins among others. Once vascular endothelium is exposed to ionizing radiation, proteins contained within storage reservoirs in endothelial cells are transported to the cell membrane, where they can serve as receptors for radiation-targeted drug delivery.^{11,13,33}

Tumor microvascular endothelium that has been exposed to radiation expresses many receptors that can be identified and targeted, including molecules in the selectin family.¹⁴ These molecules are expressed on leukocytes (L-selectin), endothelial cells (E-selectin, P-selectin), and platelets (P-selectin). These cell adhesion molecules are known for mediating leukocyte rolling on endothelial cells and platelet–leukocyte aggregation.^{7,23,26} Studies have shown that elevated levels of selectins are present in the serum of subjects experiencing an inflammatory state.³⁰ P-selectin, in particular, is an important disease marker as it plays an essential role in many inflammatory processes including cancer, coronary artery disease, stroke, and diabetes.^{23,30} It is also a valuable target for drug delivery because it is radiation-inducible, and its cellular expression is rapid and reversible.^{14,17} Due to its increased expression on endothelial cells, its potential as a vascular target for tumor imaging and therapy has been proposed in this study.

Radiation Induced P-Selectin

Radiation therapy is used to treat approximately 60% of patients with cancer.¹⁴ Ionizing radiation induces the expression of cell adhesion molecules and other proteins in tumor microvasculature.¹⁴ Targeting radiation-induced neoantigens on tumor microvasculature is a valuable approach for site-specific delivery of cytotoxic drugs, radiosensitizers and therapeutic radionuclides. We hypothesized that radiation-induced neoantigens such as P-selectin can be targeted with antibodies for tumor imaging and targeted drug delivery to cancer. Such an approach can enhance the effects of cancer treatment beyond that of radiation alone.

P-selectin (also designated as CD62P) is a 140 kD integral glycoprotein originally found on the surface of activated platelets (giving rise to the designation P-selectin) and later on endothelial cells.^{26,27} It is sequestered in storage vesicles in the form of α -granules in platelets and Weibel-Palade bodies in endothelial cells.^{7,14} Upon exposure to ionizing radiation, P-selectin expression is stimulated and these secretory granules fuse with the cell membrane.¹⁴ Typically, this expression can also be induced by the presence of various cytokines including

histamine, thrombin, tumor necrosis factor alpha (TNF α) and lipopolysaccharide.¹⁴ Once P-selectin is expressed on the surface of endothelial cells, it is rapidly internalized by endocytosis. Its general structure consists of an amino-terminal lectin domain, EGF-like domain, a variable number of short consensus repeat units, followed by a carboxyl-terminus.²⁶

After radiation exposure, P-selectin is transiently expressed on the vascular endothelial cells in the lumen of the vasculature, and once inflammation has subsided, it moves back to the cell interior.¹⁴ This transient expression enables the identification of a particular window of time during which targeting the tumor microvasculature can be particularly effective (see Fig. 1). This approach can be used to target both therapeutic and imaging agents to the radiation-treated tumor. In our study, we specifically examined the role of antibodies targeted to radiation-induced P-selectin in tumor microvasculature. This method of targeting tumors is significant because antibodies can be produced to specifically bind P-selectin, which can then be conjugated to drugs and other therapeutics for radiation-guided drug delivery.

Therapeutic Antibodies

The use of therapeutic antibodies as a treatment for cancer began with the discovery of the structure of antibodies and the development of hybridoma technology.^{2,25} These advances provided the first reliable source of monoclonal antibodies (mAbs), and allowed for the specific targeting of many different types of tumors. Monoclonal antibodies have been used in oncologic applications since the late 1990s with the development of rituximab (Rituxan), trastuzumab (Herceptin), and gemtuzumab (Mylotarg).² Since then, there has been an increase in the number of targeted antibody therapies available. Most of these therapies are based on whole, intact mAbs. While providing therapeutic value, these mAbs often exhibit slow clearance from the blood compartment to the tumor and are often too large to sufficiently penetrate the tumor tissue, thus limiting the efficacy of this type of therapy.^{22,37} The Fc domain in these intact mAbs can also bind to cellular receptors and slow clearance times, creating systemic side effects.³⁷

One alternative to these problems has been the genetic engineering of antibody fragments such as single chain fragment variable (scFv) antibodies. These antibody fragments are comprised of immunoglobulin heavy chain and light chain variable regions that are connected by a short peptide linker. These antibody fragments retain the specific antigen-binding affinity of the parent mAb, while reducing some of the disadvantages associated with mAbs. Some of these advantages include their relatively small size (~30 kD), which enables them to penetrate tumors more rapidly and increase renal clearance rates, and also their lack of an Fc domain which makes them less immunogenic.^{3,8,22,37} These advantages make scFv antibodies potentially useful for both tumor imaging and therapy.

Radionuclides have also been used in combination with therapeutic mAbs to either increase therapeutic activity or exploit the targeting properties of the mAbs for cancer imaging.^{28,29} Antibodies against tumor associated antigens have been used as targeting moieties to deliver cytotoxic radionuclides to tumor cells.^{28,29} Radionuclide-bearing mAbs used in the clinic include Zevalin and Bexxar, both anti-CD20 mAbs radiolabelled with ⁹⁰Y and ¹³¹I, respectively.^{28,29}

The selection and characterization of anti-human P-selectin scFvs is a first step towards the construction of cancer imaging or new anticancer antibodies designed for optimal blood clearance and tumor penetration. However, very few recombinant antibodies are available to study the clinical function of P-selectin except for therapeutic attempts in the form of monoclonal antibodies and chimeric antibodies.^{10,15,19,32,34} Presently, there have not been any studies using P-selectin as an imaging target in cancer, partly due to the lack of specific

desired antibodies to the protein. For these reasons, the aim of this study is to develop anti-human P-selectin scFvs that can be used for radiation-guided tumor imaging.

Tumor Imaging

The ability to non-invasively visualize P-selectin targeting *in vivo* would allow us to understand the biodistribution and pharmacokinetics of antibody-conjugated drugs and radionuclides targeted to tumors. In this manner, tumor growth can be monitored and effectiveness of therapy can be evaluated. In this study, anti-P-selectin scFv antibodies have been labeled with fluorescent optical probes and radionuclides for near-infrared optical imaging and gamma camera imaging of P-selectin expression in radiation treated lung tumor xenografts. Tumor targeting efficacy and *in vivo* kinetics profiles were observed and evaluated using complementary optical and nuclear imaging modalities.

Nuclear imaging modalities such as PET, SPECT and gamma camera imaging typically exhibit high sensitivity in deep tissues, and increased spatial resolution but poor temporal resolution as compared to optical imaging.^{18,20} Optical imaging modalities have the advantage of higher temporal resolution, safer use since they do not use ionizing radiation or radioactive materials, but they provide lower spatial resolution and sensitivity in deep tissues.^{4,5,16,35,38} A major limitation of optical imaging is the high absorption and scattering that occurs in biological tissues and the limited penetration of the light through the body. Near-infrared fluorescence (NIR) imaging is a particular kind of optical imaging that exploits the near-infrared range in the spectra to bypass the typical absorption and autofluorescence problems seen in optical imaging of biological tissues.^{4,35} Typically, tissues exhibit a high photon absorbance in both the visible wavelength range (350–650 nm) and the infrared range (above 900 nm).⁴ However, in the NIR range of 650–900 nm the absorbance of water and tissues in the body is at a minimum and thus allows photons to penetrate tissue more efficiently and minimizes scattering.^{4,5,16,35,38} Functional imaging of molecularly based events such as tumor-specific binding can be performed using both nuclear and optical imaging modalities in order to provide complementary information.^{6,24,31} In this study, fluorescent probes in the NIR range were conjugated to anti-P-selectin scFvs for NIR optical imaging, and complementary data was gathered using ¹¹¹In labeled anti-P-selectin scFvs with gamma camera imaging.

METHODS

Drug delivery methods generally rely on the use of targeting agents to deliver the conjugate to the appropriate site, and therapeutic agents to create the desired therapeutic effect at that site. In order to create optimal drug delivery vehicles, biodistribution and kinetics of the targeting agent and its receptor must first be studied and validated. Optical imaging and nuclear imaging are commonly used for these purposes and provide complementary information regarding targeting kinetics and biodistribution. This section focuses on the methods used for preliminary imaging studies in order to explore the potential of P-selectin targeting for radiation-guided drug delivery.

Antibody Selection

All antibodies were screened from phage display libraries and developed in the Molecular Recognition Core Laboratory at Vanderbilt University. The antibodies with highest affinity for P-selectin were then selected for *in vitro* and *in vivo* imaging studies presented here. The modified antibody used in the nuclear imaging studies was developed in collaboration with Dr. Martin Brechbiel in the radiochemistry laboratory at the National Institutes of Health.

In vitro Model

Immunofluorescence Assay—Primary culture human umbilical vein endothelial cells (HUVECs) were cultured till 80% confluency in Lab-Tek II chamber slide wells (Nunc International, Naperville, IL) in endothelial cell medium and incubated 37 °C in a humidified 5% CO₂ atmosphere. Cells were then incubated with human TNF α (500 mM) or treated with 3 Gy radiation for 30 min. After treatment, cells were fixed with 4% paraformaldehyde for 10 min at room temperature, and washed 3 times with antibody buffer (4 g bovine serum albumin, 0.1 g sodium azide, 0.75 g glycine, and 100 μ L PBS at a pH of 7). All wells were blocked with 200 μ L PBS containing 3% bovine serum albumin for 2 h at room temperature. Anti-P-selectin scFv (100 μ L) was added to selected wells and incubated at room temperature for 1 h in a humid chamber and then washed. The cells were incubated with 1 μ g of biotinylated anti-E-Tag monoclonal antibody for 1 h, washed 5 times with PBS-Tween solution and incubated with 10 μ L of a 1:200 dilution of FITC or Cy3 conjugated streptavidin for 1 h. The cells were washed, counterstained with DAPI, and mounted with a solution of 90% glycerol and 10% PBS-Tween. Cells were visualized with an Olympus BX60 system for fluorescence microscopy. All images were obtained at an original magnification of 40 \times and imported and analyzed using Adobe Photoshop 7.0.

In vivo Model

Synthesis of ScFv-Cy7 Conjugates—The synthesis of Cy7-scFv conjugates was achieved through conjugation of monofunctional Cy7-NHS ester with the ϵ -amino group of the lysine residue of the scFv antibody. The reaction was performed in a sodium bicarbonate buffer at a pH of 8. The dye to scFv ratio was calculated to be 1:1. All scFv were labeled according to Amersham Biosciences protocol for labeling with Cy dye NHS esters. The resulting conjugates were purified using a gel desalting column (G-25, Pierce). The yields of Cy7-scFv conjugates were typically over 80%.

Synthesis of ¹¹¹In-DTPA-scFv10Acys Conjugates—In order to radiolabel scFv 10A with ¹¹¹In, a chelator (CHX-A" DTPA) was used for enhanced *in vivo* stability of the radionuclide.³⁶ To enable conjugation of scFv 10A to CHX-A" DTPA, a cysteine residue was engineered into the amino acid sequence of the scFv. The synthesis of ¹¹¹In-CHX-A" DTPA-scFv10Acys conjugate was achieved through conjugation of scFv 10Acys-CHX-A" DTPA with ¹¹¹In using thiol chemistry of the cysteine residue. The reaction was performed by adding 5 μ L of ¹¹¹InCl₃ (3 mCi) to the scFv 10Acys-CHX-A" DTPA conjugate in 120 μ L of sodium citrate (1 M) buffer (pH 5) and incubating at room temperature for 1 h. The resulting conjugate was purified using a gel desalting column (G-25, Pierce). The yields of ¹¹¹In-CHX-A" DTPA-scFv10Acys conjugate were typically over 70% as measured by thin layer chromatography.

Cell Culture—Lewis lung carcinoma (LLC) cells were obtained from American Type Culture Collection (Manassas VA, USA) and were cultured at 37 °C in a humidified atmosphere containing 5% CO₂ in Dulbecco's modified eagle medium supplemented with 10% fetal bovine serum and 1% penicillin streptomycin solution.

Animal Models—Animal studies were performed according to a protocol approved by Vanderbilt's IACUC. Male athymic nude mice (nu/nu) between four to six weeks old (Harlan Inc., Indianapolis IN, USA) were anesthetized using a ketamine and xylazine solution before being injected subcutaneously in the right and left hind legs with 1 \times 10⁶ LLC cells suspended in 100 μ L sterile phosphate buffered saline. Ten days after inoculation, the tumors reached an approximate size of 0.5–0.6 cm in diameter, and the mice were used for *in vivo* imaging studies.

Statistical Analysis—One-way analysis of variance (ANOVA) was used for statistical evaluation. Means were compared by using Student's *t*-test. A *p*-value of <0.05 was considered significant.

Radiation Treatment—Mice were irradiated with 300 kV X-rays using a Pantak Therapax DXT 300 Model X-ray unit (Pantak, East Haven, CT) using an adjustable collimator set to limit dosage to the tumor region only. The animals were anesthetized using ketamine and xylazine solution prior to irradiation to inhibit mobility during treatment. The left hind limb was irradiated at a dose of 6 Gy and the right hind limb was treated with sham radiation at a dose of 0 Gy. During irradiation procedures, 1 cm thick lead blocks were arranged above the rest of the body, leaving only the desired area on the hind limb exposed for treatment.

Optical Imaging

In vivo NIR Fluorescence Imaging—*In vivo* NIR fluorescence imaging was performed with a Xenogen IVIS 200 small animal imaging system (Xenogen Inc., Alameda CA, USA) with a Cy7 filter set (excitation at 680 nm and emission at 775 nm). Nude mice bearing Lewis lung carcinoma tumors implanted in both hind limbs were treated with radiation. The tumor on the left side of each mouse received a radiation dose of 6 Gy and the tumor on the right side received no radiation (sham radiation dose of 0 Gy) and served as an internal negative control. Three hours following radiation, mice were anesthetized using an intraperitoneal injection of ketamine and xylazine and prepared for tail vein injections of the scFv-Cy7 conjugates. The experimental group consisted of 3 mice receiving 50 μ g of scFv 10A-Cy7, and the control group consisted of 3 mice receiving 50 μ g of scFv 4A-Cy7.

At 1, 4, and 8 h post-injection, all mice were anesthetized with isoflurane and imaged with the Xenogen IVIS. The surface fluorescence intensity of each animal was measured and normalized. All fluorescence images were acquired with 1 s exposure time using an *f*/stop of 2. Following imaging at the final time point, mice were immediately euthanized by inhalation of carbon dioxide, and their tumors and major organs were excised and prepared for *ex vivo* imaging. The total fluorescence flux (p/s/cm²/sr) for each organ was measured. For quantitative comparison, regions of interest (ROIs) were drawn over tumors and normal tissues and the results were presented as mean \pm standard deviation (SD) for a group of three animals.

Nuclear Imaging

In vivo Gamma Camera Imaging—*In vivo* gamma camera imaging was performed with an Elscint Apex SP-6HR gamma camera using a medium energy parallel hole collimator. Mice (*n* = 3 for each ¹¹¹In-CHX-A" DTPA-scFv conjugate) were anesthetized with ketamine/xylazine solution and injected via tail vein with 500 μ Ci of ¹¹¹In-CHX-A" DTPA-scFv conjugate containing 50 μ g scFv each. Planar images were taken every 24 h after injection of the ¹¹¹In-CHX-A" DTPA conjugated scFv antibody for 10 days. Static digital images were collected for 10 min each in a 512 \times 512 matrix, with typical counts around 500,000 at the 24-h imaging time and fewer counts with each subsequent imaging session. All images were processed using ImageJ software provided by the NIH. Following imaging of the final time point, mice were immediately euthanized by inhalation of carbon dioxide, and their tumors and major organs were excised and individually labeled for well counts. The total counts for each organ were measured using a Capintec radioisotope calibrator CRC-10R. For quantitative comparison, regions of interest (ROIs) were drawn over tumors and normal tissues in the planar images, and the results were presented as mean \pm standard deviation (SD) for a group of three animals.

RESULTS AND DISCUSSION

In vitro Results

To determine whether scFv 10A bound to P-selectin *in vitro*, HUVECs were treated with human TNF α to stimulate P-selectin expression on the cell membrane before being incubated with FITC labeled antibody. During immunofluorescent microscopy of the treated cells, it was observed that scFv 10A antibody bound to P-selectin protein on the cell membrane of cells treated with TNF α 30 min after treatment (Fig. 2). Control scFv antibody did not show significant antibody binding to P-selectin on the cell membrane (Fig. 2).

To confirm whether scFv 10A bound to P-selectin *in vitro*, HUVECs were treated with ionizing radiation to stimulate P-selectin expression on the cell membrane before being incubated with antibody. Cells were stained with DAPI nuclear stain (blue) and scFv 10A was conjugated with Cy3 dye (red). During immunofluorescent microscopy of the treated cells, it was observed that scFv 10A antibody bound to P-selectin protein on the cell membrane of cells treated with a radiation dose of 3 Gy 30 min after treatment (Fig. 3). ScFv10A antibody did not show significant binding to cells treated with sham radiation of 0 Gy (Fig. 3).

In vivo Model Results

Optical Imaging—To determine whether scFv 10A bound to P-selectin *in vivo*, nude mice with Lewis lung carcinoma xenografts were treated with radiation before receiving antibody. Near-infrared (NIR) fluorescence imaging studies were performed in order to evaluate the tumor targeting ability of scFv 10A as compared to control antibody scFv 4A (Fig. 4). Specific targeting was seen with scFv 10A to the tumor treated with 6 Gy (left leg) as compared to untreated tumor (right leg) and the rest of the body as early as 4 h post-injection (Fig. 4). Mice treated with scFv 4A did not show tumor-specific binding, with considerable antibody still circulating in the kidneys at 4 h post-injection.

The antibody biodistribution in the animal was tracked using near-infrared imaging at 4 h after injection. Fluorescence intensity of different regions of interest (ROI) was created by quantifying photons emitted per second for each desired area. The ratios of irradiated tumor, control tumor and the rest of the body per kilogram of body weight are shown (Fig. 5). The ratio of fluorescence intensity of the irradiated tumor to the control tumor is approximately 25:1, and the ratio to the rest of the body is over 100:1. In order to confirm tumor binding of scFv 10A, tumors were excised and imaged *ex vivo* (Fig. 6). The irradiated tumor shows significantly more fluorescence intensity as compared to the unirradiated control tumor.

Nuclear Imaging—To evaluate the P-selectin targeting ability of scFv 10A *in vivo*, and validate the results observed in the near-infrared fluorescence imaging studies, gamma camera imaging studies were performed using the gamma-ray emitting radionuclide ^{111}In . In order to do this, a chelator (CHX-A" DTPA) was used to sequester the ^{111}In and enhance stability *in vivo*.³⁶ The scFv 10A antibody was also modified to contain a cysteine residue (scFv 10Acys) in order to allow conjugation of the CHX-A" DTPA chelated ^{111}In .

To determine whether scFv 10Acys bound to P-selectin *in vivo*, nude mice bearing Lewis lung carcinoma tumors were treated with the tumor on the left side of each animal receiving a radiation dose of 6 Gy and the tumor on the right side receiving an intratumoral injection of TNF α as an internal positive control. Negative controls consisted of mice with tumors that were treated with no radiation (sham radiation dose of 0 Gy). Three hours following radiation, ^{111}In -CHX-A" DTPA conjugated scFv 10Acys was injected into both groups of mice.

Beginning 24 h after injection all mice were imaged on a gamma camera imaging system, and every 24 h after for up to 10 days (or approximately 3 half-lives for the ^{111}In). Specific targeting was seen with scFv 10Acys to the tumor treated with 6 Gy (left leg) and the tumor treated with TNF α (right leg) as compared to untreated control tumors. Binding was observed at 24 h and continued for up to 10 days post-injection. Figure 7 shows a representative image of ^{111}In -CHXA" DTPA conjugated scFv 10Acys targeting a Lewis lung carcinoma tumor treated with 6 Gy 10 days after injection.

Figure 8 below shows a higher percentage (> 10%) of binding activity in tumors treated with 6 Gy radiation than tumors treated with TNF α . Binding activity dropped approximately 30% in radiation-treated tumors over a period of 10 days. Binding activity in TNF α treated tumors decreased approximately 45% over 10 days. Both radiation-treated and TNF α treated tumors showed increased tumor binding activity over tumors treated with sham radiation of 0 Gy.

ScFv 10Acys binds tumors *in vivo* treated with both radiation and TNF α treatment for up to 10 days post-injection (Fig. 9). However, radiation produced greater P-selectin binding than TNF α . Tumor binding was nearly five times higher in radiation treated tumors as compared to untreated tumors. Tumor binding remained constant for up to 2 days before steadily decreasing up to 10 days. As expected, percent uptake was highest in the liver, followed by radiation treated tumor, kidneys, bladder, TNF α treated tumor, and untreated tumor. Liver, kidney and bladder uptake decreased by approximately half over a time period of 10 days.

DISCUSSION

Expression of P-selectin in tumor vascular endothelium after exposure to ionizing radiation enables the preferential delivery of labeled anti-P-selectin scFv antibodies to irradiated tumors. Previous studies with radiolabeled scFv demonstrated the site-specific localization of the antibodies in the targeted tumor vascular cells. In our study, we described the selective targeting of scFv antibodies to tumor microvascular endothelial cells *in vitro*. We also showed selective antibody targeting to tumors *in vivo* using two methods: NIR fluorescence imaging and gamma camera imaging.

The binding of labeled scFv antibody to P-selectin in tumor microvascular endothelial cells was tested using human umbilical vein endothelial cells (HUVECs). These cells were treated with TNF α , a potent stimulator of P-selectin, and were incubated in the presence of scFv antibody. Immunostaining showed antibody binding all over the cell membrane, consistent with the observed location of P-selectin after TNF α and radiation treatment.¹⁴ Staining of cell membranes was not present when scFv not specific to P-selectin (control scFv) was used. Immunofluorescence confirms that scFv 10A antibody selectively binds to HUVECs expressing P-selectin and does not bind to other cells. Therefore, we have shown that scFv 10A antibody is specific to human P-selectin expressed on the surface of vascular endothelial cells *in vitro*. To confirm antibody targeting and binding to tumor vascular endothelial cells *in vivo*, a heterotopic lung tumor model was used in mice and binding was visualized with near-infrared (NIR) and gamma camera imaging.

Near-infrared (NIR) imaging is a useful non-invasive tool for visualizing tumor targeting *in vivo*, and a powerful complement to nuclear imaging techniques. NIR imaging has the advantages of using neither ionizing radiation nor radioactive materials, and is becoming a more important tool for imaging of animals in preclinical models. Fluorescent probes, such as Cy7, allow the visualization of anatomical, functional and molecular events in small animals. These attributes make it ideal for studying the molecular target P-selectin and its role in tumor vasculature. With better understanding of tumor angiogenesis, it is possible to develop P-selectin targeted therapies. To achieve this, imaging studies with both NIR and nuclear

techniques were performed and tumor targeting to P-selectin was studied. NIR fluorescence imaging was performed using a Cy7-conjugated scFv antibody, and gamma camera imaging was performed using an ^{111}In -CHX-A" DTPA-conjugated scFv antibody modified to include a cysteine residue for conjugation purposes. Combining both optical imaging and nuclear imaging techniques enabled the confirmation of results using complementary imaging modalities.

Optical imaging techniques such as NIR fluorescence imaging take advantage of recent developments in fluorescent probes in the near-infrared region of the spectrum. Conjugation of Cy7, a fluorescent probe with excitation at 680 nm and emission at 775 nm, did not have significant effect on the optical properties of Cy7 dye and did not affect the receptor binding affinity or specificity of the scFv antibodies to P-selectin. Since NIR fluorescence intensity is a function of optical path length between excitation light and the subject, subcutaneous tumor models were chosen for this study. Imaging was done both *in vivo* and *ex vivo* with excised tumors in order to validate signal detected in *in vivo* images. As expected, fluorescence intensity was lesser *in vivo* as compared to direct imaging of excised tissues. Other researchers have noted similar observations when imaging with and without skin and detected an attenuation of fluorescence intensity by approximately 44%.³⁸ This is most likely caused by the loss of excitation and emission light by penetration of the skin, in addition to scattering caused by the skin. Because of these issues, gamma camera imaging was used to minimize the effects of skin scattering on imaging of tumor binding.

In vivo NIR fluorescence imaging of mice with irradiated and unirradiated tumors given Cy7-labeled scFv 10A and 4A showed significant targeting of irradiated tumors using scFv 10A as early as 4 h post treatment. Binding in tumors was measured to be over 25 times higher than in unirradiated tumors and over 100 times higher than the rest of the body. Direct imaging of excised tumors confirmed these results with significant binding in irradiated tumors as compared to unirradiated tumors. Tumor binding was not observed in animals treated with scFv 4A.

In order to further study the kinetics of this scFv antibody, the antibody was modified to include a cysteine residue for conjugation to DTPA and was then radiolabeled with ^{111}In , a gamma emitter. This modified antibody construct was used to image mice with irradiated tumors, TNF α treated tumors and unirradiated tumors. The ionizing gamma rays emitted from the ^{111}In penetrated through the tumor and surrounding layers of skin, providing greater sensitivity with gamma camera imaging as compared to NIR fluorescence imaging. *In vivo* imaging showed significant accumulation of radiolabelled scFv 10Acys in irradiated tumor tissue as compared to TNF α treated tumors, unirradiated tumors and the rest of the body for up to 10 days post-injection. Our data show that scFv 10Acys selectively targets P-selectin *in vivo* as induced with both radiation and TNF α treatment at 10 days post-injection. However, radiation produced greater P-selectin binding than TNF α . Tumor binding was nearly five times higher in radiation treated tumors as compared to untreated tumors, again suggesting antibody binding to be higher in P-selectin expressing tumors. Biodistribution of the scFv 10Acys antibody showed highest uptake in the liver (due to processing by macrophages), followed by radiation treated tumor, kidneys, bladder, TNF α treated tumor, and untreated tumor.

FUTURE WORK

Imaging P-selectin targeting *in vivo* provides a stepping stone to achieving radiation-guided drug delivery to P-selectin expressing tumors *in vivo*. Follow up work in this area would include the investigation of therapeutic radionuclides and compatible chelators that could be linked to the identified antibody scFv 10A. Effects on tumor growth must be studied over time to determine if this approach produces therapeutic effects. In addition, safety and toxicity studies

must be done to determine the effects of these radionuclides on vital organs over time. Targeted drug delivery to P-selectin in irradiated tumors should be studied using chemotherapeutic and radiosensitizing drugs commonly used in radiation therapy. Combining tumor imaging with targeted drug delivery would enable important parameters such as biodistribution, pharmacokinetics and bioavailability to be studied in greater detail. By using the targeting capability of antibodies, and exploiting the side-effects of radiation therapy, it is possible to target and treat tumors locally with both radiation and chemotherapeutic drugs much more effectively.

CONCLUSIONS

In this study we have demonstrated the successful non-invasive *in vivo* targeting of an antibody to radiation-inducible neoantigen P-selectin, in a heterotopic Lewis lung carcinoma model by using near-infrared fluorescence imaging and gamma camera imaging. In our preliminary optical imaging study, it was observed that tumor-specific binding was seen as early as 4 h post-injection. Binding in irradiated tumors was over 25 times higher than in unirradiated tumors and over 100 times higher than the rest of the body. It was also shown that scFv 10A binds P-selectin in TNF α and radiation treated HUVECs *in vitro*. Gamma camera imaging showed that the modified scFv 10A also showed successful targeting to P-selectin with tumor binding lasting for up to 10 days post-injection. Therefore, radiation-guided targeting of P-selectin for the tumor-specific delivery of therapeutic drugs and radionuclides *in vivo* is a feasible approach.

ACKNOWLEDGMENTS

This work was supported in part by National Cancer Institute grants R01-CA1256757, R21-CA128456, R01-CA112385, P30-CA68485, the Ingram Charitable Trust, and the Vanderbilt-Ingram Cancer Center. The research of Todd E. Peterson, Ph.D. was supported in part by a Career Award at the Scientific Interface from the Burroughs Wellcome Fund. This research was supported in part by the Intramural Research Program of the NIH, National Cancer Institute, Center for Cancer Research.

REFERENCES

1. Barcellos-Hoff MH, Park C, Wright EG. Radiation and the microenvironment—tumorigenesis and therapy. *Nat. Rev. Cancer* 2005;5:867–875. [PubMed: 16327765]
2. Brekke OH, Sandlie I. Therapeutic antibodies for human diseases at the dawn of the twenty-first century. *Nat. Rev. Drug Discov* 2003;2:52–62. [PubMed: 12509759]
3. Carter P. Improving the efficacy of antibody-based cancer therapies. *Nat. Rev. Cancer* 2001;1:118–129. [PubMed: 11905803]
4. Chen X, Conti PS, Moats RA. *In vivo* near-infrared fluorescence imaging of integrin $\alpha_v\beta_3$ in brain tumor xenografts. *Cancer Res* 2004;64:8009–8014. [PubMed: 15520209]
5. Cheng Z, Wu Y, Xiong Z, Gambhir SS, Chen X. Near-infrared fluorescent RGD peptides for optical imaging of integrin $\alpha_v\beta_3$ expression in living mice. *Bioconjugate Chem* 2005;16:1433–1441.
6. Dharmarajan S, Schuster DP. Molecular imaging of the lungs. *Acad. Radiol* 2005;12:1394–1405. [PubMed: 16253851]
7. Dole VS, Bergmeier W, Mitchell HA, Eichenberger SC, Wagner DD. Activated platelets induce Weibel-Palade-body secretion and leukocyte rolling *in vivo*: role of P-selectin. *Blood* 2005;106(7):2334–2339. [PubMed: 15956287]
8. Fang J, Jin H, Song J. Construction, expression and tumor targeting of a single-chain Fv against human colorectal carcinoma. *World J. Gastroenterol* 2003;9(4):726–730. [PubMed: 12679920]
9. Geng L, Osusky K, Konjeti S, Fu A, Hallahan D. Radiation-guided drug delivery to tumor blood vessels results in improved tumor growth delay. *J. Control. Release* 2004;99(3):369–381. [PubMed: 15451595]

10. Gu J, Liu Y, Xia L, Wan H, Li P, Zhang X, Ruan C. Construction and expression of mouse–human chimeric antibody SZ-51 specific for activated platelet P-selectin. *Thromb. Haemost* 1997;77(4): 755–759. [PubMed: 9134655]
11. Hallahan DE, Geng L, Cmelak AJ, Chakravarthy AB, Martin W, Scarfone C, Gonzalez A. Targeting drug delivery to radiation-induced neoantigens in tumor microvasculature. *J. Control. Release* 2001;74:183–191. [PubMed: 11489494]
12. Hallahan D, Geng L, Qu S, Scarfone C, Giorgio T, Donnelly E, Gao X, Clanton J. Integrin-mediated targeting of drug delivery to irradiated tumor blood vessels. *Cancer Cell* 2003;3:63–74. [PubMed: 12559176]
13. Hallahan DE, Qu S, Geng L, Cmelak A, Chakravarthy A, Martin W, Scarfone C, Giorgio T. Radiation-mediated control of drug delivery. *Am. J. Clin. Oncol* 2001;24(5):473–480. [PubMed: 11586099]
14. Hallahan DE, Virudachalam S. Accumulation of P-selectin in the lumen of irradiated blood vessels. *Radiat. Res* 1999;152:6–13. [PubMed: 10381836]
15. He XY, Xu Z, Melrose J, Mullowney A, Vasquez M, Queen C, Vexler V, Klingbeil C, Co MS, Berg EL. Humanization and pharmacokinetics of a monoclonal antibody with specificity for both E- and P-selectin. *J. Immunol* 1998;160(2):1029–1035. [PubMed: 9551944]
16. Hsu AR, Hou LC, Veeravagu A, Greve JM, Vogel H, Tse V, Chen X. *In vivo* near-infrared fluorescence imaging of integrin $\alpha_v\beta_3$ in an orthotopic glioblastoma model. *Mol. Imaging Biol* 2006;8:315–323. [PubMed: 17053862]
17. Kneuer C, Ehrhardt C, Radomski MW, Bakowsky U. Selectins—potential pharmacological targets? *Drug Discov. Today* 2006;11:1034–1040. [PubMed: 17055414]
18. Kundu BK, Stolin AV, Pole J, Baumgart L, Fontaine M, Wojcik R, Kross B, Zorn C, Majewski S, Williams MB. Tri-modality small animal imaging system. *IEEE Trans. Nucl. Sci* 2006;53(1):66–70.
19. Kurome T, Katayama M, Murakami K, Hashino K, Kamihagi K, Yasumoto M, Kato I. Expression of recombinant mouse/human chimeric antibody specific to human GMP-140/P-selectin. *J. Biochem. (Tokyo)* 1994;115(3):608–614. [PubMed: 7520038]
20. Li C, Wang W, Wu Q, Ke S, Houston J, Sevic-Muraca E, Dong L, Chow D, Charnsangavej C, Gelovani JG. Dual optical and nuclear imaging in human melanoma xenografts using a single targeted imaging probe. *Nucl. Med. Biol* 2006;33:349–358. [PubMed: 16631083]
21. Lin PC. Optical imaging and tumor angiogenesis. *J. Cell. Biochem* 2003;90:484–491. [PubMed: 14523982]
22. Lin MZ, Teitell MA, Schiller GJ. The evolution of antibodies into versatile tumor-targeting agents. *Clin. Cancer Res* 2005;11:129–138. [PubMed: 15671537]
23. Lorant DE, Topham MK, Whatley RE, McEver RP, McIntyre TM, Prescott SM, Zimmerman GA. Inflammatory roles of P-selectin. *J. Clin. Invest* 1993;92(2):559–570. [PubMed: 7688760]
24. Lyons S. Advances in imaging mouse tumour models *in vivo*. *J. Pathol* 2005;205:194–205. [PubMed: 15641018]
25. McCarron PA, Olwill SA, Marouf WMY, Buick RJ, Walker B, Scott CJ. Antibody conjugates and therapeutic strategies. *Mol. Interv* 2006;6(2):368–380.
26. McEver RP. Selectins. *Curr. Opin. Immunol* 1994;6(1):75–84. [PubMed: 7513527]
27. McEver RP. Regulation of function and expression of P-selectin. *Agents Actions Suppl* 1995;47:117–119. [PubMed: 7540351]
28. Milenic DE, Brady ED, Brechbiel MW. Antibody-targeted radiation cancer therapy. *Nat. Rev. Drug Discov* 2004;3:488–498. [PubMed: 15173838]
29. Milenic DE, Brechbiel MW. Targeting of radio-isotopes for cancer therapy. *Cancer Biol. Therapy* 2004;3(4):361–370.
30. Molenaar TJM, Twisk J, de Haas SAM, Peterse N, Vogelaar BJCP, van Leeuwen SH, Michon IN, van Berkel TJC, Kuiper J, Biessen EAL. P-selectin as a candidate target in atherosclerosis. *Biochem. Pharmacol* 2003;66:859–866. [PubMed: 12948867]
31. Neves AA, Brindle KM. Assessing responses to cancer therapy using molecular imaging. *Biochim. Biophys. Acta* 2006;1766:242–261. [PubMed: 17140737]

32. Tsurushita N, Fu H, Melrose J, Berg EL. Epitope mapping of mouse monoclonal antibody EP-5C7 which neutralizes both human E- and P-selectin. *Biochem. Biophys. Res. Commun* 1998;242(1): 197–201. [PubMed: 9439635]
33. Wachsbarger P, Burd R, Dicker AP. Tumor response to ionizing radiation combined with antiangiogenesis or vascular targeting agents: exploring mechanisms of interaction. *Clin. Cancer Res* 2003;9:1957–1971. [PubMed: 12796357]
34. Walter UM, Ayer LM, Wolitzky BA, Wagner DD, Hynes RO, Manning AM, Issekutz AC. Characterization of a novel adhesion function blocking monoclonal antibody to rat/mouse P-selectin generated in the P-selectin-deficient mouse. *Hybridoma* 1997;16(3):249–257. [PubMed: 9219035]
35. Wu Y, Cai W, Chen X. Near-infrared fluorescence imaging of tumor integrin $\alpha_v\beta_3$ expression with Cy7-labeled RGD multimers. *Mol. Imaging Biol* 2006;8:226–236. [PubMed: 16791749]
36. Wu C, Kobayashi H, Sun B, Yoo TM, Paik CH, Gansow OA, Carrasquillo JA, Pastan I, Brechbiel MW. Stereochemical influence on the stability of radio-metal complexes *in vivo*. Synthesis and evaluation of the four stereoisomers of 2-(p-nitrobenzyl)-trans-CyDTPA. *Bioorg. Med. Chem* 1997;5:1925–1934. [PubMed: 9370037]
37. Wu AM, Senter PD. Arming antibodies: prospects and challenges for immunoconjugates. *Nat. Biotechnol* 2005;23(9):1137–1146. [PubMed: 16151407]
38. Zaheer A, Lenkinski RE, Mahmood A, Jones AG, Cantley LC, Frangioni JV. *In vivo* near-infrared fluorescence imaging of osteoblastic activity. *Nat. Biotechnol* 2001;19:1148–1154. [PubMed: 11731784]

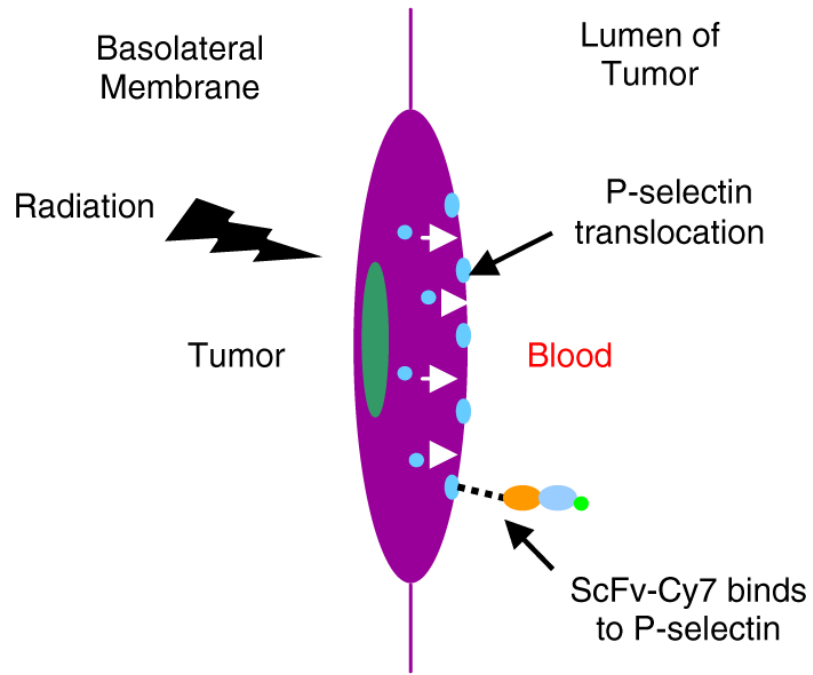


FIGURE 1. Schematic of endothelial cell response to ionizing radiation. Ionizing radiation causes P-selectin located in Weibel-Palade bodies to translocate from the interior of the cell to the luminal side of the cell and fuse with the cell membrane.

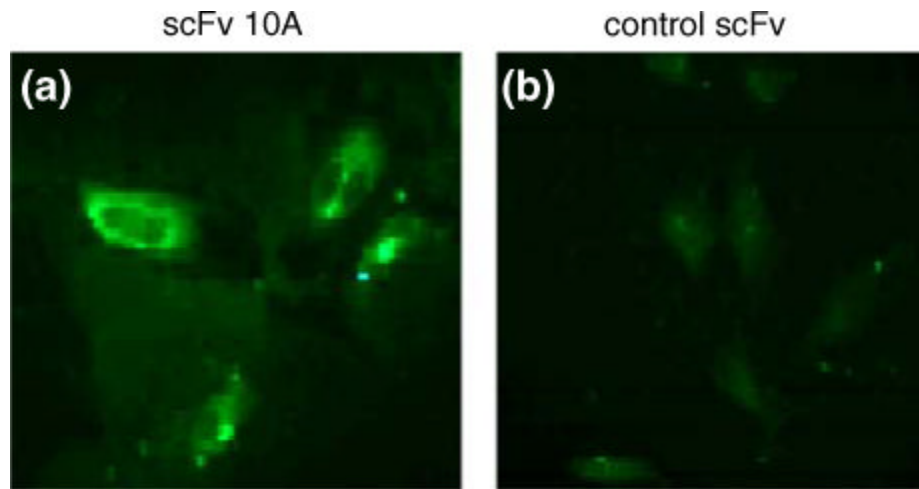


FIGURE 2. Immunofluorescent microscopy of antibody binding to P-selectin in HUVECs treated with $TNF\alpha$. (a) HUVECs stained with scFv 10A-FITC. (b) HUVECs stained with control scFv-FITC.

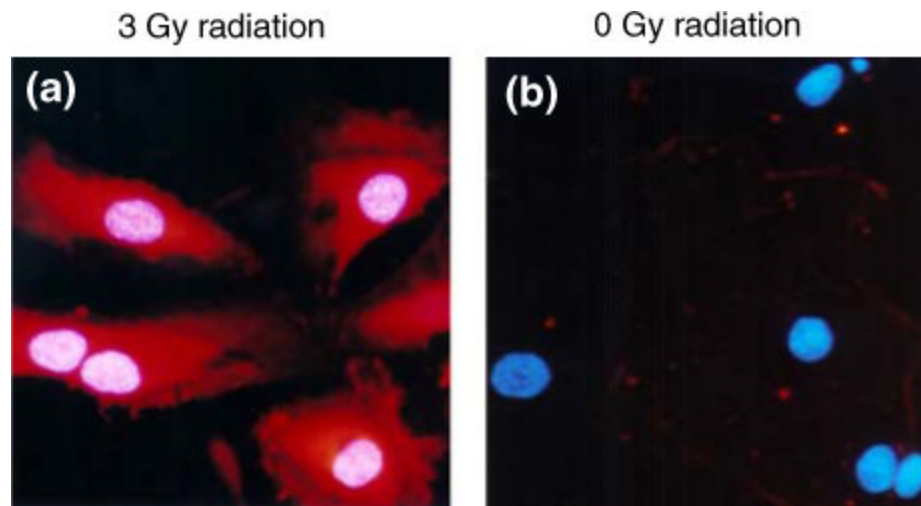


FIGURE 3. Immunofluorescent microscopy of antibody binding to P-selectin in HUVECs treated with radiation. Cells were stained with DAPI nuclear stain (blue) and scFv 10A was conjugated with Cy3 dye (red). (a) scFv 10A binding to P-selectin on HUVECs treated with a radiation dose of 3 Gy. (b) No scFv 10A binding in HUVECs treated with a sham radiation dose of 0 Gy.

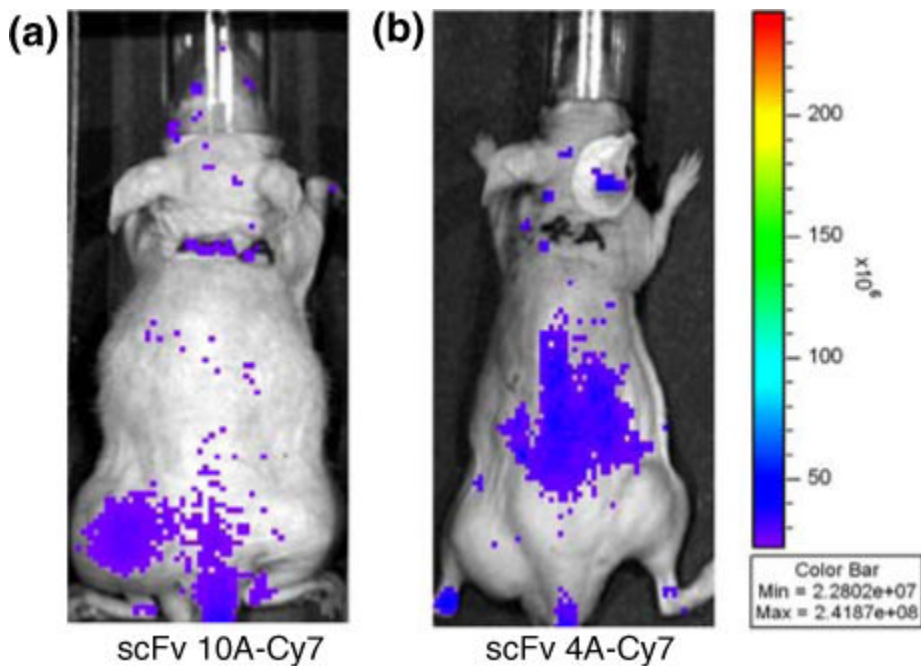


FIGURE 4. NIR imaging of *in vivo* scFv biodistribution at 4 h post-injection. (a) Specific targeting was seen with scFv 10A to the tumor treated with 6 Gy (left leg) as compared to untreated tumor (right leg) and the rest of the body as early as 4 h post-injection. (b) No tumor-specific binding seen with mice treated with scFv 4A.

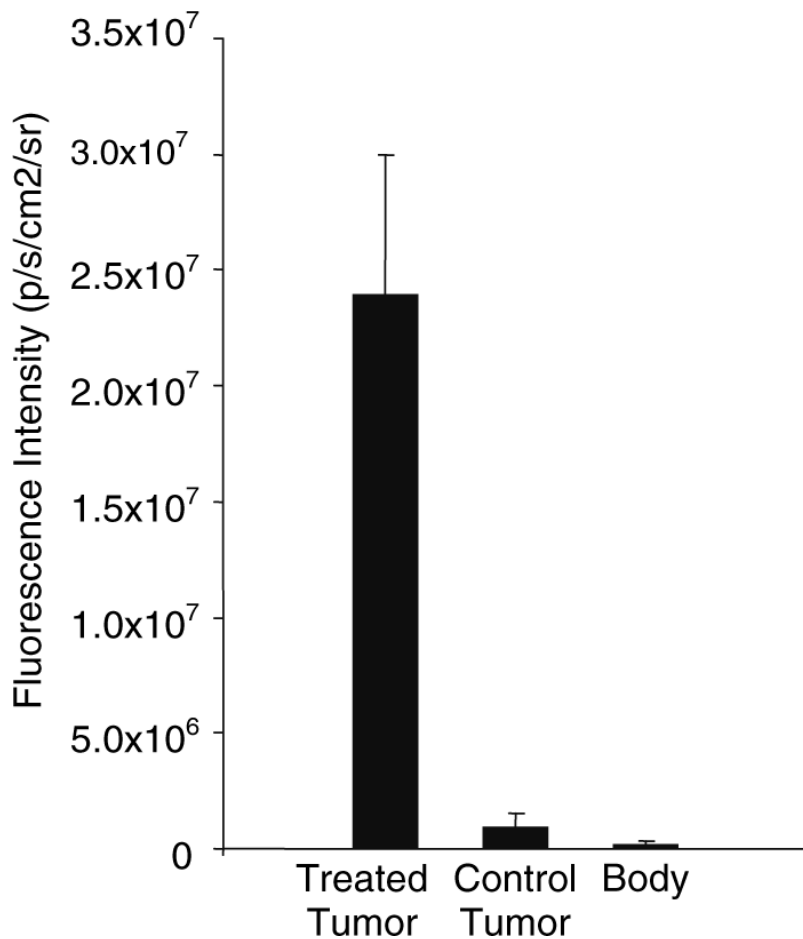


FIGURE 5. Graph of tumor to body ratios from NIR imaging. The ratios of irradiated tumor, control tumor and the rest of the body per kilogram of body weight are shown. The ratio of fluorescence intensity of the irradiated tumor to the control tumor is approximately 25:1, and the ratio to the rest of the body is over 100:1.

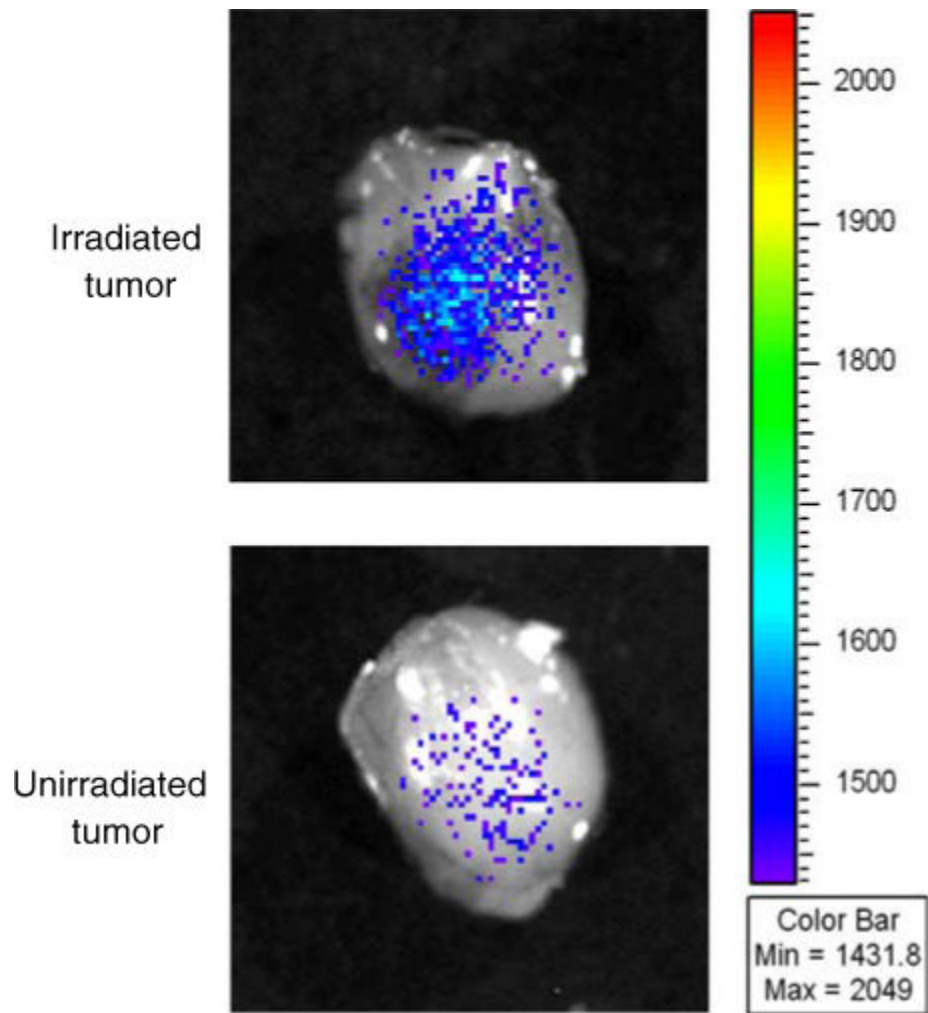


FIGURE 6. NIR imaging of *ex vivo* scFv 10A in tumors treated with and without radiation at 4 h post-injection. The irradiated tumor shows significantly more fluorescence intensity as compared to the unirradiated control.

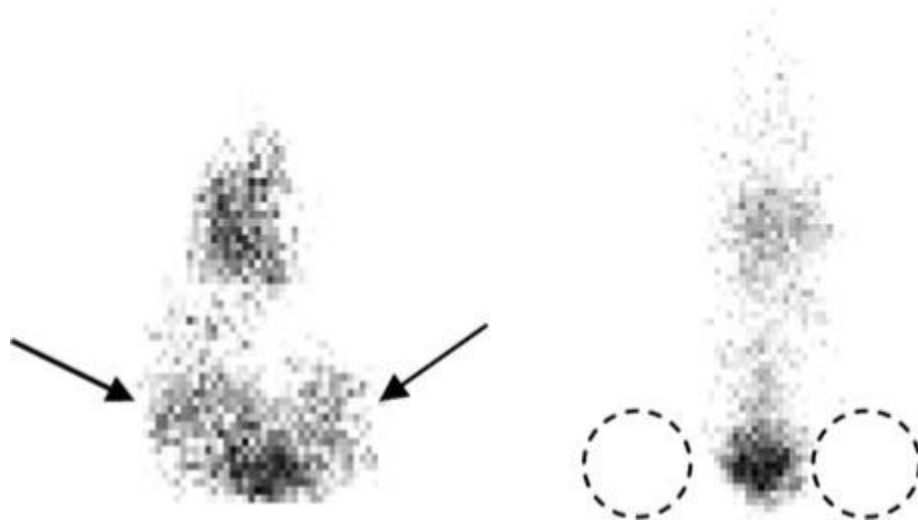


FIGURE 7.

Gamma camera imaging of *in vivo* scFv biodistribution at 10 days post-injection. Mice were imaged on a gamma camera imaging system at 24 h post-injection and every 24 h after for up to 10 days (or approximately 3 half-lives for the ^{111}In). Mouse on the left side has left hind limb tumor treated with 6 Gy radiation, and right hind limb tumor treated with $\text{TNF}\alpha$ (positive control). Mouse on the right side has left and right hind limb tumors treated with sham radiation dose of 0 Gy (as negative control). Specific targeting was seen with scFv 10Acys to the tumor treated with 6 Gy and the tumor treated with $\text{TNF}\alpha$ as compared to untreated control tumors.

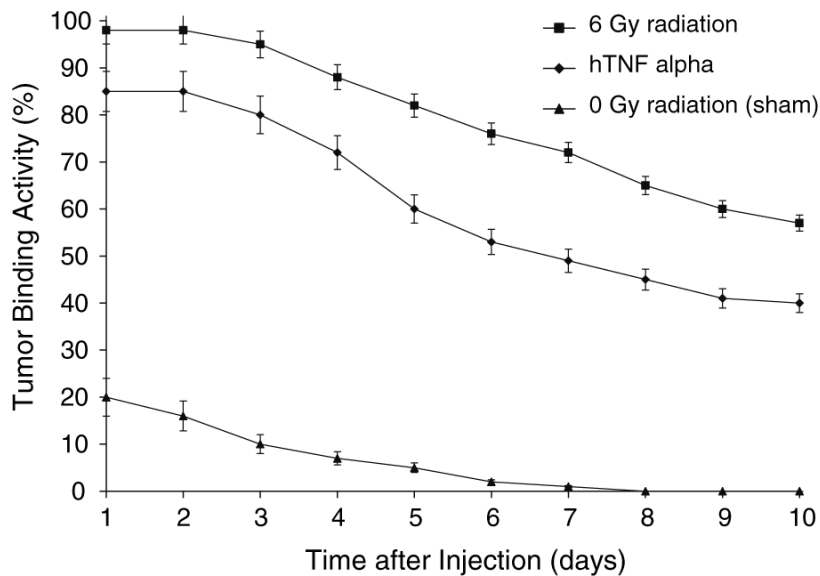


FIGURE 8. Tumor binding activity of three different treatments as measured with a gamma camera. Tumors treated with 6 Gy radiation show a higher percentage (> 10%) of binding activity than tumors treated with TNF α . Both radiation treated and TNF α treated tumors showed increased tumor binding activity over tumors treated with sham radiation of 0 Gy.

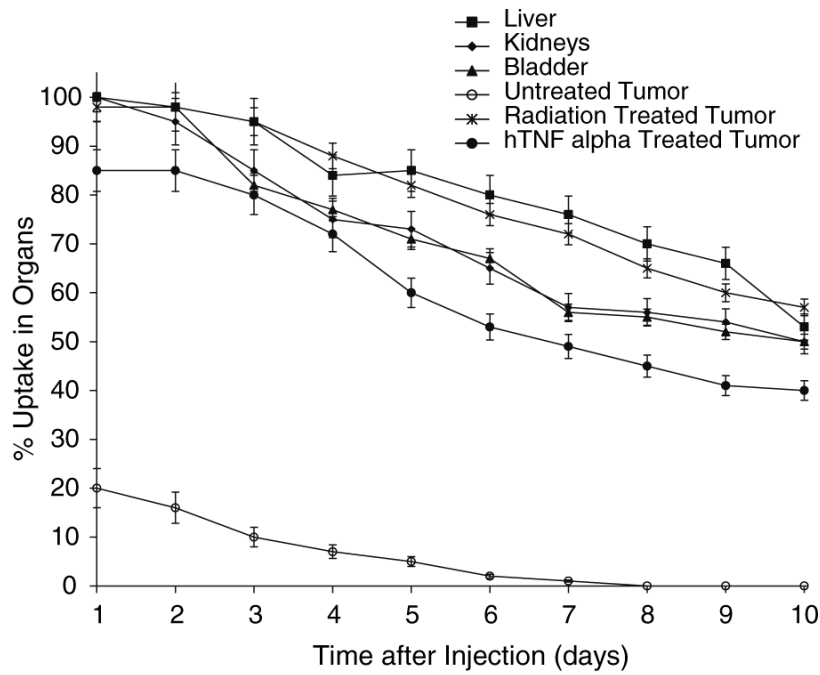


FIGURE 9. Percent uptake of ¹¹¹In-CHX-A'' DTPA-scFv 10Acys in various organs over 10 days after injection as measured with a gamma camera. ScFv 10Acys binds tumors treated with both radiation and TNF α treatment for up to 10 days post-injection. Tumor binding was nearly five times higher in radiation treated tumors as compared to untreated tumors.